Fuzzy controller hardware implementation for an EV's HESS energy management

Original Scientific Paper

JBARI Hatim

Moulay Ismaïl University,
National High School of Arts and Crafts of Meknes (ENSAM-Meknès),
Team of Modelling, Information Processing and Control Systems (MPICS)
B.P. 15290 EL Mansour Meknes 50500, Meknès, Morocco
ha.jbari@edu.umi.ac.ma

ASKOUR Rachid

Moulay Ismaïl University,
National High School of Arts and Crafts of Meknes (ENSAM-Meknès),
Team of Modelling, Information Processing and Control Systems (MPICS)
B.P. 15290 EL Mansour Meknes 50500, Meknès, Morocco
r.askour@umi.ac.ma

BOUOULID IDRISSI Badr

Moulay Ismaïl University,
National High School of Arts and Crafts of Meknes (ENSAM-Meknès),
Team of Modelling, Information Processing and Control Systems (MPICS)
B.P. 15290 EL Mansour Meknes 50500, Meknès, Morocco
b.bououlid@umi.ac.ma

Abstract – *The recent technological advances related to embedded systems, and the increased requirements of the Electric Vehicle (EV) industry, lead to the evolution of design and validation methodologies applied to complex systems, in order to design a product that respects the requirements defined according to its performance, safety, and reliability. This research paper presents a design and validation methodology, based on a hardware-in-the-loop (HIL) approach, including a software platform represented by Matlab/Simulink and a real-time STM32 microcontroller used as a hardware platform. The objective of this work is to evaluate and validate an Energy Management System (EMS) based on Fuzzy Logic Controller (FLC), developed in C code and embedded on an STM32 microcontroller. The developed EMS is designed to control, in real-time, the energy flow in a hybrid energy storage system (HESS), designed in an active topology, made of a Li-ion battery and Super-Capacitors (SC). The proposed HESS model was organized using the Energetic Macroscopic Representation (EMR) and constructed on Matlab/Simulink software platform. The evaluation and validation of the developed algorithm were performed by comparing the HIL and simulation results under the New European Driving Cycle (NEDC).*

Keywords: *Fuzzy Logic Controller, Hardware-In-the-Loop, Hybrid Energy Storage System, STM32 microcontroller*

1. INTRODUCTION

All around the world, the transportation sector is the main contributor to urban pollution [1]. Public health studies in different countries have demonstrated that the increase in air pollution concentrations is associated with an increase in the mortality rate, particularly in urban areas. The electric vehicle (EV) seems to be an efficient solution to overcome this public health problem, a technology that is encouraged by government policies, to support and generalize this means of transport that ensures zero-CO_2 emissions. Meanwhile, several manufacturers have focused a large part of their development program on this industrial segment, with the aim of accelerating the total insertion of the EV in the car fleet during the next years.

Therefore, EVs are currently facing several challenges, especially those related to the range and lifetime of the main source of energy provided by batteries [2]. In fact, industrial companies and scientists are confronted with the challenge of finding solutions to EV's

limitations, taking into account the constraints related to its performance required by the users. In this case, the adoption of a *HESS*-based architecture with the integration of *SCs* [3,4], and the implementation of an *EMS* ensuring efficient energy management between energy sources, allowing optimization of the efficiency of the battery lifespan and the vehicle autonomy.

According to the literature, *EMS* is a key element to optimize the EV battery lifespan and autonomy. Indeed, there are three main approaches to energy management algorithms: *EMS*-based optimization algorithms, algorithms based on artificial intelligence, and rule-based algorithms [5,6,7]. The authors in [8,9] propose a rule-based *EMS*, applied to the management of the energy flow in a *HESS* in a full-active topology [10], ensuring the supply of the EV's powertrain. The *EMS* presented in this work is based on a Fuzzy Logic Controller (FLC), which supports two inputs represented by the SC's state of charge and the power ratio related to the maximum battery power. Thus, the objective of this study is to control the *SCs* as an energy buffer, and to support the power pulses, in order to improve the battery performance and optimize its lifespan. Another work presented in [11], uses a fuzzy controller that supports the same inputs mentioned previously. This work ensures the same objectives with the criterion of minimizing the Root Mean Square (RMS) of the battery current. In [12], the authors present a work that is based on two fuzzy controllers, managing the distribution of the power demanded by the powertrain, between the battery and the *SCs* in a *HESS*'s full-active topology. The first fuzzy controller supports the estimated source's states of charge using the Kalman filter, the energy sources, and the required power. The second one determines the power required by the battery, where the inputs are based on the power calculated by the first block of the fuzzy controller, and the power estimated via the Kalman filter. The objective of this work is to minimize the power pulses that the battery should support.

On the other hand, the evolution of EVs has to take into account constraints related to costs and development times, in order to optimize the time to market of this technology. Hence, the rise of new methodologies and platforms, designed to satisfy these requirements, has been able to optimize the design of complex systems such as the EV, for instance, the Hardware-In-the-Loop (*HIL*) applied to *EMS*s. Thus, some researchers in [13] have proposed a *HIL* architecture for the emulation and real-time control of a boost converter, designed in the PSIM software, with a PI cascaded controller on the STM32 microcontroller, to regulate the output voltage. The objective of this work is to evaluate the control model through the comparison of the *HIL* results, and the simulation model established in the PSIM software. In [14] the authors present another *HIL* architecture based on a real-time simulator of an EV, built using the Simulink platform, and a vehicle control unit (VCU) designed on a hardware platform. The EV model is made of a BLDC engine with a motor control unit (MCU), and a *HESS* powering the vehicle. The VCU is connected to the simulator through inputs/outputs (CAN bus, RS232, analog/digital I/O) using a DSP interface. Another *HIL* simulation platform applied to the electric vehicle powertrain used to emulate the driving cycle is presented in [15]. The proposed architecture is based on two coupled electrical machines, the first one is an induction machine that emulates the vehicle's traction machine and the second one is a DC machine that provides the load simulation. A dSPACE DS1102 board is used as an interface between the control established on the Simulink platform, and the power converter assures the control of both machines. The authors in [16,17] present a solution of *HIL* that aims at the validation of an FLC-based *EMS* algorithm, designed for the control of the energy flow in a *HESS* in a full-active topology, built on the Simulink platform. The Atmega microcontroller was used in the first work, while the FPGA hardware platform was used in the second work for the same architecture.

Thus, this paper presents a *HIL* architecture based on an active-topology *HESS* model, organized using the Energetic Macroscopic Representation (EMR) and implemented on the Matlab/Simulink software platform. The proposed *HESS* is designed to supply an EV to ensure a maximum speed of 120km/h with a propulsion power of 70kW. The electric vehicle can provide a total range of 150km. The *HESS*'s *EMS* is used for the management and optimization of the energy flow using an FLC. The proposed FLC was developed in C language, and embedded in the STM32 microcontroller. The STM32 is connected in a closed loop with the *HESS* simulation model, to control in real-time, the contribution of both sources: *SCs* and battery.

In a previous work [16], an architecture of a *HESS* is presented. The proposed *EMS* based on FLC is implemented on an Atmega microcontroller. The output of the used FLC is defined by a simplified method for computing the Center of Gravity (*CoG*) abscissa of the resulting polygon. The FLC is based on a 3x3 rule base matrix. In this work, the rule-based *EMS*-FLC is embedded in the STM32 low-power microcontroller, which is a part of the family of ARM-based 32-bit microcontrollers and has some major hardware advantages over the Atmega microcontrollers 8-bit. It's also popular and widely used in the field of EVs. Moreover, the *CoG* defuzzification method is based on a precise value depending on the fuzzy set's center of gravity of the resulting area. In addition, the proposed FLC is based on a 4x5 rule base matrix.

Indeed, the objective of this work is to evaluate on the one hand, the performance of the developed *EMS*, on the other hand to validate the algorithm of the *EMS*-FLC, via the comparison between the results obtained from the *HIL* and the simulation.

The rest of this paper is organized as follows: section 2 presents the nomenclature; the description of the model and the control of the developed *HESS* is detailed in section 3. Section 4 presents the proposed *HESS*. Section 5 details the *EMS* implementation methodology in the STM32 microcontroller. Section 6 presents and discusses the experimental and simulation results. Finally, Section 7 concludes the paper.

2. NOMENCLATURE

C_{SC}	SC Capacitance (F)
CoG	Center Of Gravity
E_{bat}	Battery energy
EMS	Energy Management System
$HESS$	Hybrid Energy Storage System
HIL	Hardware-In-the-Loop
i_{bat}	battery current (A)
i_{bat_ref}	battery current reference (A)
i_{ch_bat}	DC–DC battery Current converter (A)
i_{ch_sc}	DC–DC SC Current converter (A)
i_{DC}	DC BUS Current (A)
i_{req_ref}	HESS Current reference (A)
i_{sc}	SC current (A)
i_{sc_ref}	SC current reference (A)
k_{cont}	Battery contribution factor
P_{bat_Fil}	Filtered battery power reference
P_{bat_lim}	Battery power limit
P_{req}	Required drivetrain power (W)
R_{ESR}	SC Equivalent Series Resistance
$RMSE$	Root Mean Square Error
SC	Supercapacitors
SoC_{sc}	SC State of Charge (%)
U_{bat}	battery voltage (V)
U_{bat_meas}	Measured battery voltage (V)
U_{DC}	DC BUS voltage (V)
U_{ch_bat}	DC–DC battery voltage converter (V)
U_{ch_SC}	DC–DC SC voltage converter (V)
U_{sc}	SC voltage (V)
α_{bat}	DC–DC battery converter duty cycle
α_{sc}	DC–DC SC converter duty cycle
η_{ch_bat}	DC–DC Battery converter efficiency
η_{ch_sc}	DC–DC SC converter efficiency

3. *HESS* MODELING AND CONTROL

The developed system is a 70 kW *HESS* in full-active topology [12], shown in Fig. 1. It includes two energy sources: the primary one is represented by the Li-Ion battery and the secondary source uses the *SCs*. The 100Ah battery and the 5000F *SCs* are interfaced with the DC bus via two bidirectional buck-boost DC/DC converters and a principal coupling capacitor. The characteristics of the power sources are shown in Table 1 and Table 2. The adopted topology has the advantage of decoupling the battery and the *SCs* control, in order to control separately the power flow between the electrical sources and the DC bus voltage.
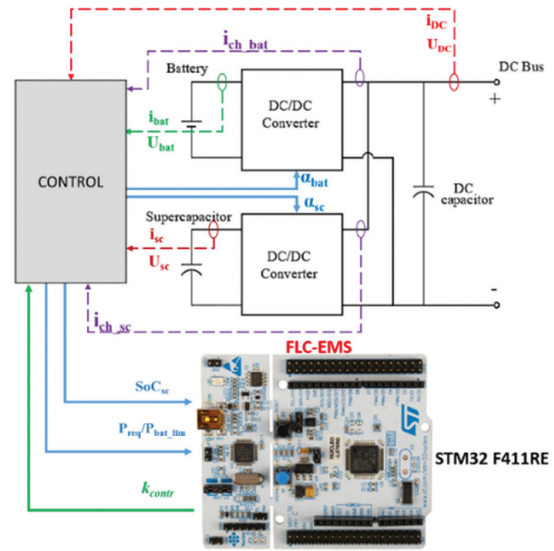
Fig. 1. Scheme of the proposed *HESS*

2.1. *HESS* MODELING

• Battery:

The complex electrochemical phenomena involved in a battery make its modeling highly complicated [18]. The simplified model adopted in this study shown in equation 1, is characterized by an internal capacity C_{bat} and an internal impedance r_{bat} of the battery pack.

$$U_{bat}(t) = r_{bat}i_{bat} + \frac{1}{C_{bat}}\int_{t_0}^{t} i_{bat}(t)\, dt \qquad (1)$$

$$SOC_{bat}(t) = SOC_{bat}(t_0) + \frac{1}{Q_{bat}}\int_{t_0}^{t} i_{bat}(t)\, dt \qquad (2)$$

The battery state of charge (equation 2) is the ratio of the battery's capacity at any given time to its total capacity. The state of charge is an important parameter to manage efficiently the battery control:

Table 1. Characteristics of the battery source

Battery Li-Ion cell (3.7V)	Symbol	Value	Unit
SoC Limits	SoC_{batt}	[30, 100]	%
Energy density	ρ_{batt}	160	Wh/kg
total mass	M_{batt}	314	Kg
energy	E_{batt}	654	Ah

- Supercapacitors (SC):

Characterized by a fast dynamic behavior, SCs have the advantage of being able to support frequent power variations during charging or discharging phases. There are several models in the literature, with variable complexity depending on the purpose of using these models. However, a simplified model has been adopted in this study, shown in equation 3, based on an internal capacitance C_{SC} and the equivalent series resistance R_{ESR}.

$$U_{SC}(t) = R_{ESR}i_{SC} + \frac{1}{C_{SC}}\int_{t_0}^{t} i_{SC}(t)\,dt \qquad (3)$$

The calculation model of the SCs state of charge in a given instant t, is presented in equation 4. The calculation model is based on the ratio of the voltage of the SCs at this moment t to its initial voltage.

$$SOC_{SC}(t) = \frac{U_{SC}(t)}{U_{SC\_init}} \qquad (4)$$

Table 2. Characteristics of the SC's source (GTCAP GTSPP-2R7-508UT)

SC (2.7V)	Symbol	Value	Unit
Capacitance	Csc	5000	F
ESR	RESR	0.21	mΩ
SoC Limits	SoCsc	[50, 100]	%

- DC-DC converter:

The technology of the DC-DC converter adopted in this work is a Buck-Boost chopper. This converter allows for ensuring a bidirectional energy flow, in order to ensure the power required by the powertrain on one side, the recharging of the energy sources on the other side, in particular during the braking phases, and the exchanges between both energy sources.

Thus, the first part of the chopper model is presented in equation 5, represented by the current smoothing inductor. This element is characterized by a capacity to store energy as magnetic energy, in order to supply it when it is required. Thus, providing a quasi-constant current profile. The inductor model is characterized by an inductance L_{source} and an internal resistance r_{source}.

$$\begin{cases} L_{bat}\frac{d}{dt}i_{bat} = U_{bat} + U_{L\_bat} + r_{L\_bat}i_{bat} \\ L_{SC}\frac{d}{dt}i_{SC} = U_{SC} + U_{L\_SC} + r_{L\_SC}i_{L\_sc} \end{cases} \qquad (5)$$

On the other hand, the switch model is presented in equations (6) and (7). The adopted approach in this case uses an average model with α_{bat} and α_{sc} representing the duty cycles of both choppers, η_{ch_bat}, and η_{ch_bat} are the efficiencies of the DC-DC converters, used in the proposed $HESS$.

$$\begin{cases} U_{L\_bat} = \alpha_{bat}\cdot U_{DC} \\ i_{ch\_bat} = \eta_{ch\_bat}\cdot\alpha_{bat}\cdot i_{bat} \end{cases} \qquad (6)$$

$$\begin{cases} U_{L\_SC} = \alpha_{SC}\cdot U_{DC} \\ i_{ch\_SC} = \eta_{ch\_SC}\cdot\alpha_{SC}\cdot i_{SC} \end{cases} \qquad (7)$$

- Sources Coupling and DC-bus capacitor:

In order to ensure continuous power supplied by both sources, the electrical coupling is required. Indeed, equation 8 shows the electrical model adopted in this case, which is based on the nodes law between both choppers controlling the power sources.

$$i_{hess} = i_{ch\_SC} + i_{ch\_bat} \qquad (8)$$

One of the most important criteria for evaluating the $HESS$ performance is the DC bus voltage, which should be constant. Thus, integrating a capacitor interfacing the $HESS$ and the powertrain allows control and minimizes the U_{DC} voltage fluctuations. Thus, the model of the capacitor is presented in equation 9 characterized by the internal capacitance C_{cpl}.

$$C_{cpl}\frac{d}{dt}U_{DC} = i_{hess} - i_{DC} \qquad (9)$$

- Load equivalent model:

In order to simplify the simulation model, and optimize the computation time. The equivalent load model is considered as a controllable current source, where the power profile is presented in Fig. 2. The required power used in the simulation is extracted from a powertrain model, with a maximum power of 70 kW. The power profile depends on the NEDC cycle speed, with a maximum value of 120 km/h.

$$i_{DC} = \frac{P_{req}}{U_{DC}} \qquad (10)$$
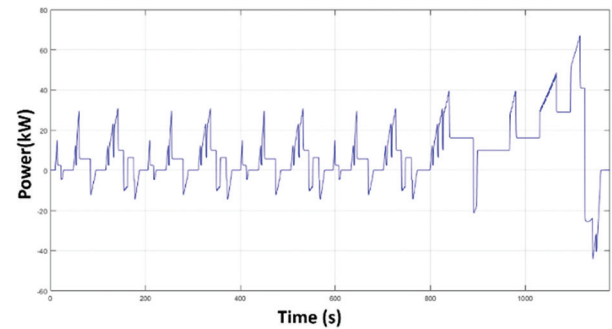
Fig. 2. Power requirement profile of the powertrain

2.2. *HESS* CONTROL

In order to design and establish the control layer, the EMR approach was adopted. The Energetic Macroscopic Representation (EMR) was developed by the Laboratory of Electrical Engineering and Power Electronics (L2EP) of Lille (France) [18, 19, 20] in the 2000s. This formalism allows to the definition of a synthetic representation for complex Multiphysics systems, respecting a functional description. It is based on integral causality and power conservation. Thus, three elements that represent the subsystems can be distinguished: source, energy accumulation, and conversion without energy accumulation. Indeed, the establishment of the control layer has been carried out based on the EMR inversion rules, in order to deduce the maximum control structure (MCS) presented in Fig. 3.
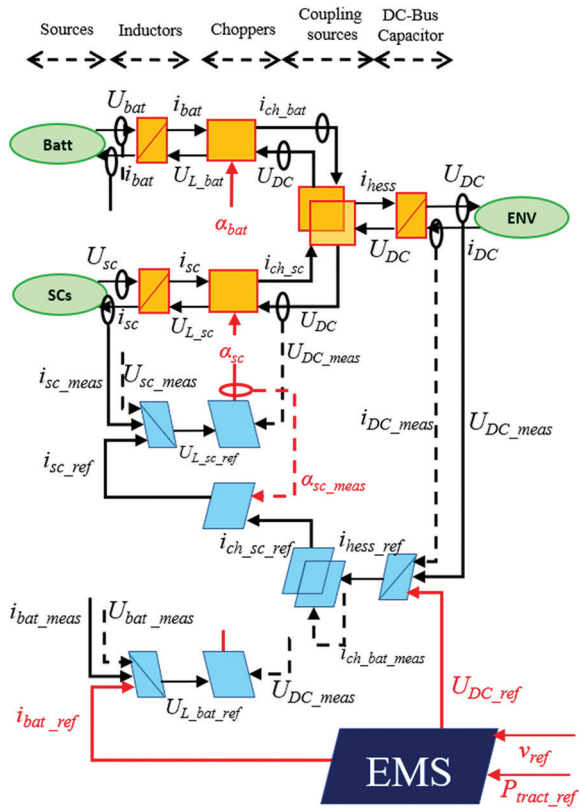
Fig. 3. EMR of the proposed *HESS*

4. ENERGY MANAGEMENT SYSTEM

The *EMS* or Energy Management System in an EV *HESS* refers to the algorithm implemented in an on-board electronic control unit, designed to ensure power management and vehicle propulsion. Hence, *EMS* represents the control strategy, which takes into account the state and model of the vehicle. The *EMS* should control the power distribution between the different energy sources, in order to minimize the solicitations which are harmful to the battery performance. It ensures the required power response respecting vehicle performance requirements (speed, stability, precision, and robustness).
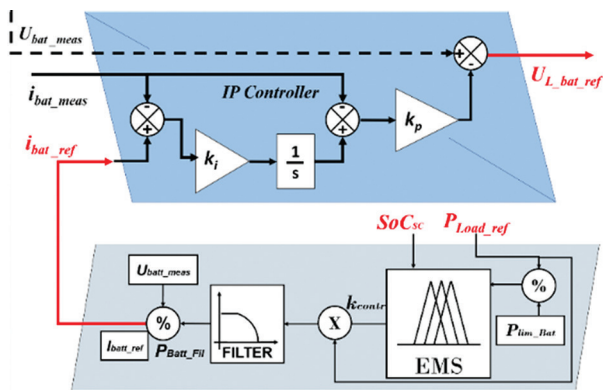
Fig. 4. *EMS* strategy scheme

In fact, this work proposes an FLC-based *EMS* (Fig. 4), providing the same objectives mentioned above.

The designed *EMS* operates according to the different phases of the vehicle driving cycle, which are summarized as follows:

- During acceleration:

In this phase, power pulses are generated, which can cause battery degradation. Indeed, the *EMS* should engage the *SCs* to support the power demand of the powertrain, since *SCs* are characterized by their fast dynamics to ensure this function, which allows to preserve the battery and optimize its lifetime.

- During quasi-constant speed:

During this phase, the *EMS* is engaging the battery progressively, to provide the powertrain demand. The *SCs* are activated to support high-frequency harmonics. This distribution is provided by the low-pass filter as shown in Fig. 4.

- During the braking phase:

In order to optimize *EV* autonomy, the braking phase is used as a source of recovered electrical energy. Thus, the *EMS* should activate the chopper of the *SCs* in order to ensure their recharge and restore them to their initial state of charge. This operation allows to the *SCs* control as an energy buffer and ensures their optimal functioning in the range of their optimal energy efficiency $SoC_{SC} \in [50,100]$ %.
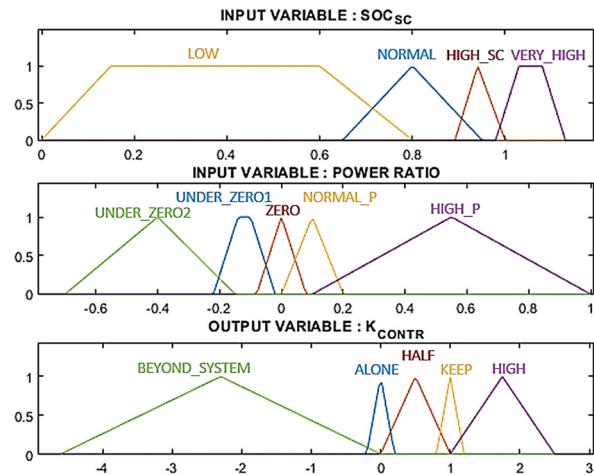
Fig. 5. Membership functions of the proposed Fuzzy Logic *EMS*

- During the total stop of the vehicle:

The architecture adopted in the proposed *HESS* allows the energetic exchange between both energy sources. Thus, during a total vehicle stop, the *EMS* should activate the battery chopper in order to recharge the *SCs*, and restore them to their initial state (when $SoC_{sc}(t) < SoC_{sc\_Init}$).

Indeed, the proposed *EMS* used to satisfy the previously mentioned objectives, is based on an *FLC-EMS*. Thus, the *EMS* output function, shown in equation 11, represents the battery contribution depending on

two input parameters that reflect the vehicle state. Therefore, the first input parameter represented by SoC_{SC} is based on four *MFs* defining the charging level of *SCs*: LOW, NORMAL, HIGH_SC, and VERY_HIGH. The second input parameter is the ratio of the required power of the *EV* powertrain to the battery power limit: $P_{Load\_ref} / P_{lim\_bat}$. This parameter allows defining the *EV* driving phases (acceleration/constant speed, deceleration/braking, vehicle total stop) according to five *MFs*: Under_ZERO2, UNDER_ZERO1, ZERO, NORMAL_P, HIGH_P.

$$k_{CONTR} = (SoC_{SC}, \frac{P_{Load\_ref}}{P_{lim\_Bat}}) \qquad (11)$$

Table 3. Inference Rules-base of the proposed FLC

POWER_ RATIO	SOC_SC			
	LOW	NORMAL	HIGH_SC	VERY_ HIGH
UNDER_ ZERO2	BEYOND-SYSTEM	BEYOND-SYSTEM	BEYOND-SYSTEM	BEYOND-SYSTEM
UNDER_ ZERO1	BEYOND-SYSTEM	ALONE	ALONE	ALONE
ZERO	HIGH	HIGH	HALF	ALONE
NORMAL_P	HIGH	KEEP	ALONE	ALONE
HIGH_P	KEEP	HALF	ALONE	ALONE

In fact, according to the literature, FLC processing includes three main steps:

- The first step is related to the input fuzzification (SoC_{SC} and $P_{Load\_ref} / P_{lim\_bat}$), represented by the membership functions (MF) of the inputs shown in Fig. 5.

- The second step is based on the inference rules (Table 1), which are constructed according to the objectives defined at the beginning of this section.

- The last step consists of defuzzification based on Mamdani's Center of Gravity (*CoG*) approach, in order to calculate the k_{CONTR} value which defines the battery's contribution. This part will be detailed in the next section.

5. *HESS HIL* DEVELOPMENT

The real-time *HIL* simulator is a validation approach that combines a hardware platform, in this case, the STM32 microcontroller, and a software simulation platform represented by the proposed Simulink model of *HESS*. The objective of this technique is the evaluation of the energy management algorithm embedded in the microcontroller. Therefore, the validation criteria are based on the control and analysis of parameters that reflect the EV performance. Fig. 6 shows the proposed *HIL* architecture, including the following elements:

- Two Simulink Models of *HESS*, organized in EMR subsystems. The first model uses the Fuzzy library block based on MFs and inference rules, which are discussed in the previous section. The second

model uses the Serial Communication blocks with a Simulink block scheme, designed to concatenate the input parameters, in order to ensure their transfer in a single frame.

- The STM32 F411RE microcontroller with 100 MHz clock frequency, connected with the computer through a USB cable via the ST-LINK debugger/programmer interface.

Fig. 6. The proposed *HESS*'s *EMS* Hardware-in-the-loop (*HIL*) architecture

In the first step of the *HIL* processing, the Simulink simulation platform of *HESS* sends both input parameters (SoC_{SC}, $P_{Load\_ref} / P_{lim\_bat}$) via the serial port. Simultaneously, the microcontroller proceeds to load the Membership functions in the predefined array structure. Once the frame is received, the first part of the program performs the extraction, assignment, and cast in the "double" data type of the input variables (SOC_{SC} et $P_{Load\_ref} / P_{lim\_bat}$).

After completing the variables loading, the algorithm performs the fuzzification function. This function allows to determine the degree of membership of each input, the mathematical model of this operation is presented in equation 12.

$$f_{dm} = \frac{(Y_{i+1}-Y_i)}{(X_{i+1}-X_i)}x + (Y_i - \frac{(Y_{i+1}-Y_i)}{(X_{i+1}-X_i)}X_i) \qquad (12)$$

Where, (X_i, Y_i) and (X_{i+1}, Y_{i+1}) are the coordinates of two points of the segments which define the MFs triangle. The input parameters (SoC_{SC} or $P_{Load\_ref} / P_{lim\_bat}$) should satisfy the condition of being in the interval defined by this segment.

Thereafter, the function of the inference rules is executed, to define the MFs value of the output parameters, based on the decision matrix which is detailed in previous work in [17]. The inference rules, in this case, are based on the logical operator "and". Each value of the MFs-outputs is defined by the minimum value of the related input values.

Once the degrees of membership of the MFs-outputs are defined, the defuzzification function is activated. This function is designed on the principle of the Center of Gravity (*CoG*) calculation. Indeed, the adopted approach is based on the decomposition of the MFs-output surfaces into independent sub-surfaces S_i (Fig. 7).

The definition of the possible configurations is performed according to the degree of membership value calculated for each MFs γ_i (Fig. 7 and Fig. 8), compared

with the intersection points of the triangle P_i representing the MFs.
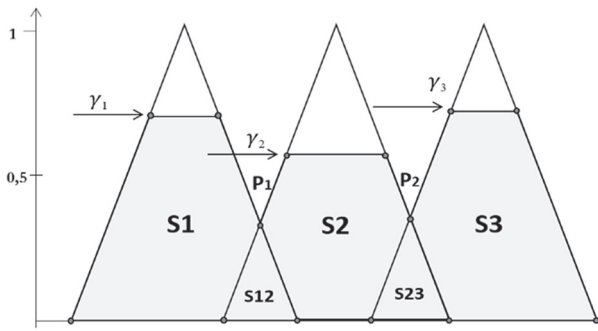
Fig. 7. Vertices of the resulting polygons ($\gamma_i > Y_P$)
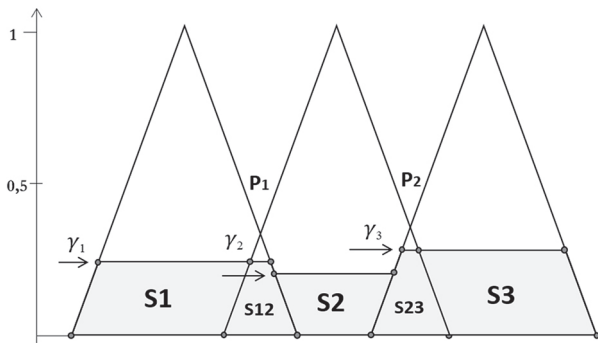
Fig. 8. Vertices of the resulting polygons ($\gamma_i < Y_P$)

Then, this operation allows for defining the configuration and coordinates of each polygon's vertices, and then the calculation of the sub-surface's (S_i) CoG which is based on equation 13:

$$\begin{cases} X_{S_i} = \frac{1}{6S_i}\sum_{j=0}^{n-1}(x_j + x_{j+1})(x_j y_{j+1} - x_{j+1}y_j) \\ S_i = \frac{1}{2}\sum_{j=0}^{n-1}(x_j y_{j+1} - x_{j+1}y_j) \end{cases} \quad (13)$$

After calculating the CoG abscissae X_i and sub-surfaces S_i, the resulting polygon CoG is calculated as follows (equation 14):

$$k_{CONTR} = \frac{1}{\sum_{i=1}^n S_i}\left(\sum_{i=1}^n (S_i X_{S_i})\right) \quad (14)$$

Thus, the resulting area CoG abscissa defines the value of the *FLC* output. It represents the battery contribution, corresponding to the input value and the inference rules established for the proposed solution. Once this value is calculated, it is submitted to the *HESS* simulation platform running on MATLAB/Simulink via the serial port, before starting a new iteration.

6. RESULTS AND DISCUSSIONS

In order to evaluate the *HESS* model and verify the proposed *FLC-EMS* algorithm, both simulation and *HIL* models were built and run in the same software platform (MATLAB/Simulink), aiming to ensure the same number of computational samples (Fig. 6). The simulations were conducted using the NEDC driving cycle

with a calculation step of 10-5. The verification of the developed algorithm was done by comparing the results of both models.

Indeed, according to the analysis of Fig. 9, the curves of SoC_{SC} and SoC_{bat} demonstrate that the *EMS* allows controlling the *SCs* as an energy buffer, and the *SCs* recover their initial SoC_{SC} at the end of each cycle $SoC_{SC}(t_{ec}) = SoC_{SC}(t_{init}) = 85\%$. Moreover, the *SCs* operate in the range that is prescribed by the *EMS*: $SoC_{SC} \in [65,86]$ %, which ensures optimal energy efficiency of the *SCs*. Whereas, the SoC_{bat} is generally smoothed and shows a limited variation. This behavior demonstrates that the battery stresses are reduced and therefore an optimization of its lifetime. Thus, according to the evaluation of the *SCs* and battery behavior, as is demonstrated by SoC_{SC} and SoC_{bat} curves in Fig. 10, the *EMS* allows the control of both sources considering the vehicle driving phases:

• *SCs* operate during acceleration phases (e.g., $t \in [10, 14]$ s, $t \in [48, 60]$ s and $t \in [117, 142.5]$ s) when power demand is fast.

• The battery supports the power demand of the powertrain during ($t \in [14, 22]$ s, $t \in [60, 84]$ s, $t \in [142.5, 154]$ s and $t \in [162, 175]$ s) when the power profile is approximately constant.

• During the braking and deceleration phases ($t \in [22, 27]$ s, $t \in [84, 95]$ s, $t \in [154, 162]$ s and $t \in [175, 187]$ s), the *EMS* engages the *SCs* to ensure their recharging from the recovered energy so that they can satisfy the next cycle demand.

• During the total stop of the vehicle ($t \in [24, 27]$ s, $t \in [84, 94]$ s and $t \in [175, 187]$ s), the SoC_{bat} decreases gradually while the SoC_{SC} increases to reach $SoC_{SC} = 85\%$. This demonstrates the possibility of the energy exchange between both sources, ensured by the adopted architecture and the implemented *EMS*.

In addition, Fig. 9 shows the behavior of the DC bus voltage U_{DC}. The analysis of the U_{DC} curve shows that the value of this parameter is relatively constant during the entire NEDC cycle: $U_{DC} = 163,25$ V with $\Delta U_{DC\_max} = 0,5$V, which demonstrates the robustness of the implemented control and the developed *EMS*. In fact, the *EMS* ensures a continuous and relatively stable power supply, without compromising the driving cycle performed by the vehicle.

• In addition, the power ratio curve shown in the same figure demonstrates that the value of the power demanded by the powertrain, is kept below the battery power limit ($P_{Load\_ref} / P_{lim\_bat} < 1$). This characteristic guarantees the reduction of battery degradation and the validity of the proposed *HESS* architecture.

• On the other hand, Fig. 9 presents the results obtained from the *HIL* simulations, allowing to validate the developed code of the *EMS-FLC* embedded in the STM32 microcontroller. Indeed, according to the comparison of the curves of the energetic

parameters presented in Fig. 9, both types of results (*HIL* and simulation) are in perfect agreement. Thus, Table 4 presents the differences calculated between both platforms, using the Root Mean Square Error

RMSE, which presents acceptable differences, due to the defined precision (10-4) in the transferred data between Matlab/Simulink and the STM32 microcontroller.

Fig. 9. Simulation results of the EV *HESS* for NEDC driving cycle [0,1180 s]

In addition, the power ratio curve shown in the same figure demonstrates that the value of the power demanded by the powertrain, is kept below the battery power limit ($P_{Load\_ref} / P_{lim\_bat} < 1$). This characteristic guarantees the reduction of battery degradation and the validity of the proposed *HESS* architecture.

On the other hand, Fig. 9 presents the results obtained from the *HIL* simulations, allowing to validate the developed code of the *EMS-FLC* embedded in the STM32 microcontroller. Indeed, according to the comparison of the curves of the energetic parameters presented in Fig. 9, both types of results (*HIL* and simulation) are in perfect agreement. Thus, Table 4 presents the differences calculated between both platforms, us-

ing the Root Mean Square Error *RMSE*, which presents acceptable differences, due to the defined precision (10^{-4}) in the transferred data between Matlab/Simulink and the STM32 microcontroller.

Table 4. *RMSE* of *HIL* and simulation energy parameters

Parameters	RMSE
SoC_{SC} (%)	$3.57 \ 10^{-2}$
SoC_{Bat} (%)	$1.8 \ 10^{-3}$
U_{DC} (V)	$2.433 \ 10^{-5}$
P_{req} / P_{lim_bat}	$2.1085 \ 10^{-17}$
Sources Contribution (%)	$12.1 \ 10^{-3}$
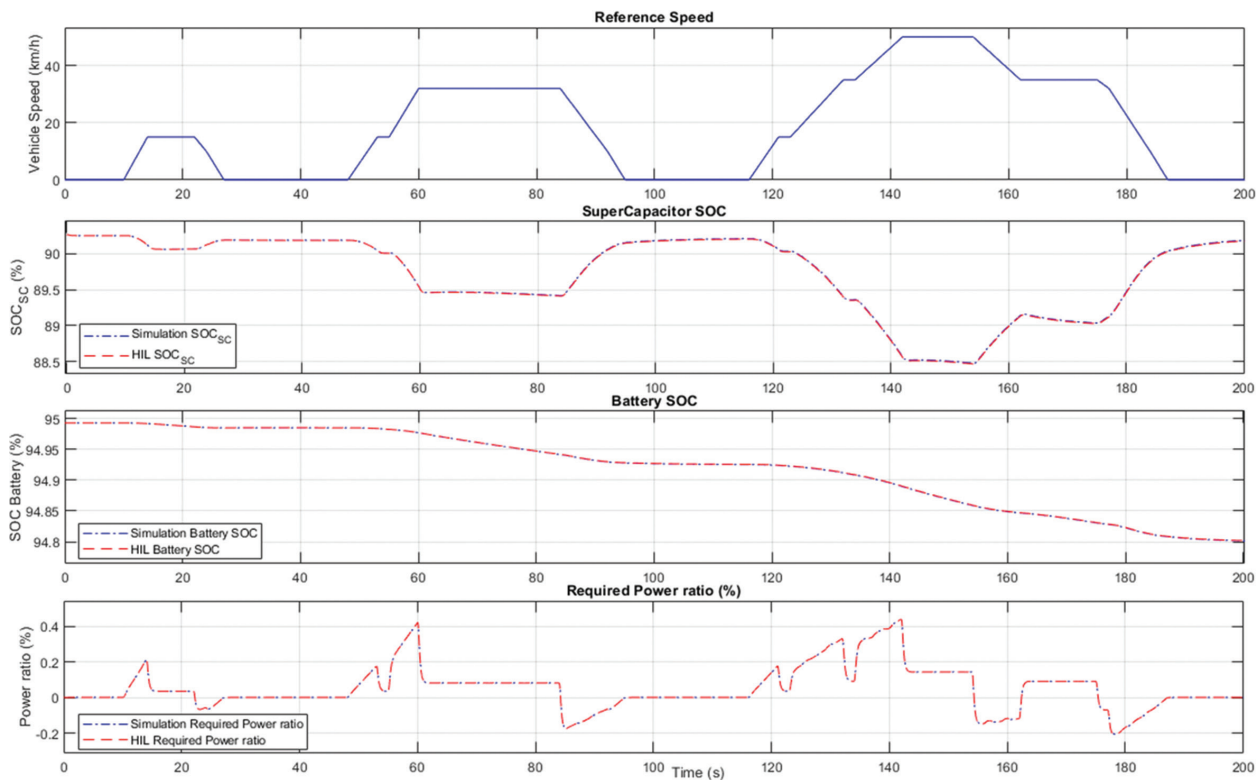
Fig. 10. Simulation results of the EV *HESS* for ECE-15 driving cycle [0,200s]

7. CONCLUSION

In this paper, a real-time *HIL* simulation for a 70kW full-active topology *HESS* is proposed. The energy management system is provided by a rule-based *EMS-FLC*, validated on MATLAB/Simulink simulation platform, developed in C code, and embedded on an STM32 microcontroller. Thus, according to the performance evaluation based on the obtained results, the developed *EMS* satisfied the conditions set for the control of both sources (*SCs* and battery), under the NEDC driving phases on the one hand. On the other hand, the comparison of the results of the energy parameters of both *HIL* and simulation platforms allowed validation of the approach adopted during the development of the proposed C code algorithm, embedded in the STM32 microcontroller.

Therefore, future research will be conducted on a real *HESS* with the same characteristics adopted in this study, using the same approach for the design of an electronic control unit ECU, integrating the control layer and communication interfaces, using the protocols applied in the EVs embedded systems, namely the Control Area Network (*CAN*).

8. REFERENCES:

[1] S. Anenberg, "A global snapshot of the air pollution-related health impacts of transportation sector emissions in 2010 and 2015", International Council on Clean Transportation, George Washington University Milken Institute School of Public Health, and the University of Colorado, Boulder, USA, p. 55.

[2] X. Zhang et al. "A novel quantitative electrochemical aging model considering side reactions for lithium-ion batteries", Electrochimica Acta, Vol. 343, 2020, p. 136070.

[3] Z. Song, J. Li, J. Hou, H. Hofmann, M. Ouyang, J. Du, "The battery-supercapacitor hybrid energy storage system in electric vehicle applications: A case study", Energy, Vol. 154, 2018, pp. 433-441.

[4] B. Yang et al. "Applications of battery/supercapacitor hybrid energy storage systems for electric vehicles using perturbation observer based robust control", Journal of Power Sources, Vol. 448, 2020, p. 227444.

[5] A. Biswas, A. Emadi, "Energy Management Systems for Electrified Powertrains: State-of-the-Art Review and Future Trends", IEEE Transactions on Vehicular Technology, Vol. 68, No. 7, 2019, pp. 6453-6467.

[6] D.-D. Tran, M. Vafaeipour, M. El Baghdadi, R. Barrero, J. Van Mierlo, O. Hegazy, "Thorough state-

of-the-art analysis of electric and hybrid vehicle powertrains: Topologies and integrated energy management strategies", Renewable and Sustainable Energy Reviews, Vol. 119, 2020, p. 109596.

[7] R. Xiong, H. Chen, C. Wang, F. Sun, "Towards a smarter hybrid energy storage system based on battery and ultracapacitor - A critical review on topology and energy management", Journal of Cleaner Production, Vol. 202, 2018, pp. 1228-1240.

[8] M. A. Silva, H. N. de Melo, J. P. Trovao, P. G. Pereirinha, H. M. Jorge, "An integrated fuzzy logic energy management for a dual-source electric vehicle", Proceedings of the 39th Annual Conference of the IEEE Industrial Electronics Society, Vienna, Austria, November 2013, pp. 4564-4569.

[9] J. P. Trovao, M. R. Dubois, M.-A. Roux, E. Menard, A. Desrochers, "Battery and SuperCapacitor Hybridization for a Pure Electric Three-Wheel Roadster", Proceedings of the IEEE Vehicle Power and Propulsion Conference, Montreal, QC, Canada, October 2015, pp. 1-6.

[10] R. S. Sankarkumar, R. Natarajan, "Energy management techniques and topologies suitable for hybrid energy storage system powered electric vehicles: An overview", International Transactions on Electrical Energy Systems, Vol. 31, No. 4, 2021.

[11] H. Jbari, M. Haidoury, R. Askour, B. Bououlid Idrissi, "Fuzzy Logic Controller for an EV's Dual-Source Hybridization", Proceedings of the 4th International Conference of Computer Science and Renewable Energies, Vol. 297, 2021, p. 01039.

[12] Z. Shengzhe, W. Kai, X. Wen, "Fuzzy logic-based control strategy for a battery/supercapacitor hybrid energy storage system in electric vehicles", Proceedings of the Chinese Automation Congress, Jinan, China, October 2017, pp. 5598-5601.

[13] D. S. Castro, R. F. Q. Magossi, R. F. Bastos, V. A. Oliveira, R. Q. Machado, "Low-Cost Hardware in the Loop Implementation of a Boost Converter",

Proceedings of the 18th European Control Conference, Naples, Italy, June 2019, pp. 423-428.

[14] C.-H. Wu, Wu-Yang Sean, Y.-H. Hung, "Development of a real-time simulator for electric vehicle with a Dual Energy Storage System", Proceedings of the 2nd International Conference on Power Electronics and Intelligent Transportation System, Shenzhen, China, December 2009, pp. 96-100.

[15] B. Tabbache, Y. Aboub, K. Marouani, A. Kheloui, M. E. H. Benbouzid, "A Simple and Effective Hardware-in-the-Loop Simulation Platform for Urban Electric Vehicles", p. 5.

[16] H. Jbari, R. Askour, B. B. Idrissi, "Real-time aTmega microcontroller-based simulator enabled hardware-in-the-Loop for fuzzy control dual-sources HESS", E3S Web Conf., Vol. 351, 2022, p. 01022.

[17] H. Jbari, R. Askour, B. B. Idrissi, "Real-time FPGA based simulator enabled Hardware-In-the-Loop for fuzzy control dual-sources HESS", International Journal of Renewable Energy Research, Vol. 12, No. 2, 2022.

[18] T. Transi, P. G. Pereirinha, A. Bouscayrol, M. Degano, "Study of Regenerative Braking Effects in a Small Electric Race Car using Energetic Macroscopic Representation", Proceedings of the International Young Engineers Forum, Costa da Caparica, Portugal, May 2019, pp. 106-111.

[19] W. Lhomme, F. Verbelen, M. N. Ibrahim, K. Stockman, "Energetic Macroscopic Representation of Scalable PMSM for Electric Vehicles", Proceedings of the IEEE Vehicle Power and Propulsion Conference, Gijon, Spain, November 2020, pp. 1-6.

[20] B.-H. Nguyen, J. P. F. Trovao, S. Jemei, L. Boulon, A. Bouscayrol, "IEEE VTS Motor Vehicles Challenge 2021 - Energy Management of A Dual-Motor All-Wheel Drive Electric Vehicle", Proceedings of the IEEE Vehicle Power and Propulsion Conference, Gijon, Spain, November 2020, pp. 1-6.